Design and Analysis of Cherenkov Radiation Detectors

Benjamin E. Chaback

Byron-Bergen High School

Advisors: Dr. J. P. Knauer and Dr. C. J. Forrest

Laboratory for Laser Energetics

University of Rochester

May 2018

Benjamin E. Chaback

1. Abstract

A Cherenkov radiation detector was designed that allows the width of the response function from neutron time of flight experiments to be reduced, resulting in more accurate ion temperature measurements of the fusing plasma in deuterium-deuterium and deuterium-tritium implosions. The width of the neutron spectrum is used to find the temperature of the plasma, which must be known to an accuracy of ~100 eV. A prototype Cherenkov-based diagnostic built at the Laboratory for Laser Energetics (LLE) consists of a reflective mirror mounted to the end of a PVC elbow connector, a reflective cone inside the detector, and a microchannel-plate photomultiplier tube on the bottom of the detector. The detector housing is made of schedule 80 PVC, a material that can be made light-tight and mitigate scattering of neutrons or muons, with the modeling of this detector being done on CAD software (OnShape). By testing the detector's response to cosmic rays, it has been determined that the detector cannot detect single particles because of the noise background. However, the detector is expected to produce a signal well above the background when used to detect the large number of neutrons that are produced from target implosions.

2. Introduction

The neutron-averaged ion temperature from a fusing plasma is determined from the variance, or width, of the 14.1 and 2.45 MeV neutron distributions. This measurement is affected by the detector response function, which is the detected signal shape from a neutron distribution with zero width. Precise measurements of the instrument response function are required to infer the ion temperature of the fusing plasma.

In current neutron time-of-flight (nTOF) diagnostics, scintillators [1] are used for detecting the primary DT (14.1 MeV) and DD (2.45 MeV) neutron peak distributions. Scintillators are materials which, when hit by a high energy particle (a neutron here), absorb the energy, exciting protons inside the scintillator. Proton recoil is used by scintillators in order to detect and measure neutron activity within the system. When these protons return to the ground state by releasing energy, the scintillator emits this energy in the form of light. Materials that emit light via scintillation have a time response that is determined by the lifetime of excited electrons in the molecular structure of the material. This results in a pulse shape with a long decay that needs to be known in order to determine the neutron distribution width and thus the ion temperature.

An alternative method to detect incident neutrons from the fusing plasma is with quartz Cherenkov detectors, which are being tested at the National Ignition Facility (NIF) [2]. A Cherenkov detector [3] is similar to a scintillator but instead of using the emitted light resulting from the particle collision, it uses the radiation created by particles moving faster than the speed of light in the medium. Neutrons excite the oxygen nucleus, producing gamma rays which in turn produce relativistic electrons through

Compton scattering. The Cherenkov light emitted from these electrons is then measured using a photomultiplier. Cherenkov radiation detectors do not emit light from electronic states and have the potential to measure the neutron energy spectrum with higher precision.

Figure 1 compares the response function of Cherenkov detectors with organic scintillators, measured at Lawrence Livermore National Laboratory (LLNL). The full width at half maximum (FWHM) is 6.6 ns for the NIF scintillator and 4.8 ns for the NIF quartz Cherenkov detector. In the work reported here, a Cherenkov radiation detector was designed and built at LLE to test these detection methods with a goal of obtaining a faster neutron response from a neutron time-of-flight signal by using Cherenkov radiation instead of excited particle energy.
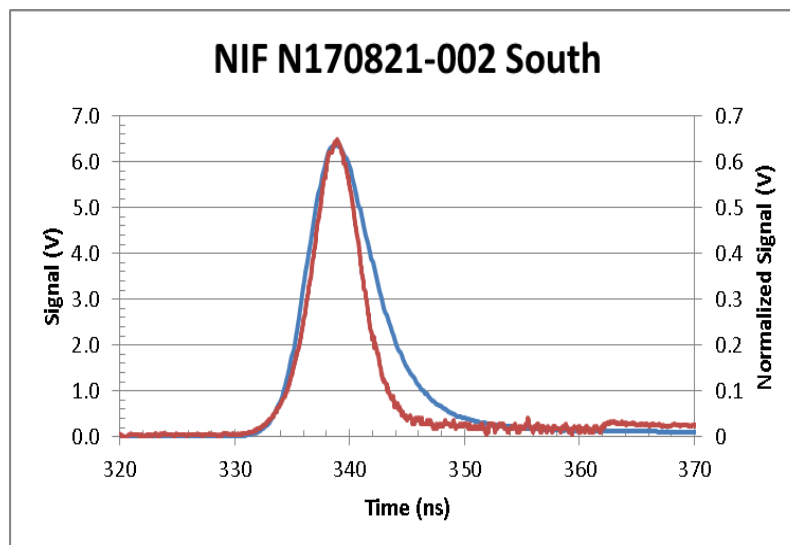
Figure 1: NIF data comparing the response function of NIF organic scintillators (blue) and NIF quartz Cherenkov detectors (red). A clear distinction in the FWHM between the different detectors is observed.

3. Cherenkov Detector

3.1 Detector design

The Cherenkov detector that was designed as shown in figure 2 had several constraints that had to be addressed before construction. For example, the detector had to be light-tight, the housing material could not be reflective, the photomultiplier tube (PMT) mount had to be easily interchangeable, and the aluminum collection mirror had to be easily accessible. The detector that was built works by allowing neutrons to enter through the light-tight threaded cap on the left and interact with the fused silica to produce Cherenkov light, which is reflected off the aluminum mirror and into the PMT. The PMT only collects the light within the reflective aluminum cone and this data is then sent to an oscilloscope where it is recorded.

Aluminum
collection mirror

Fused Silica
inside of
adaptor

Light tight threaded
cap

Reflective
aluminum cone

Photomultiplier
tube
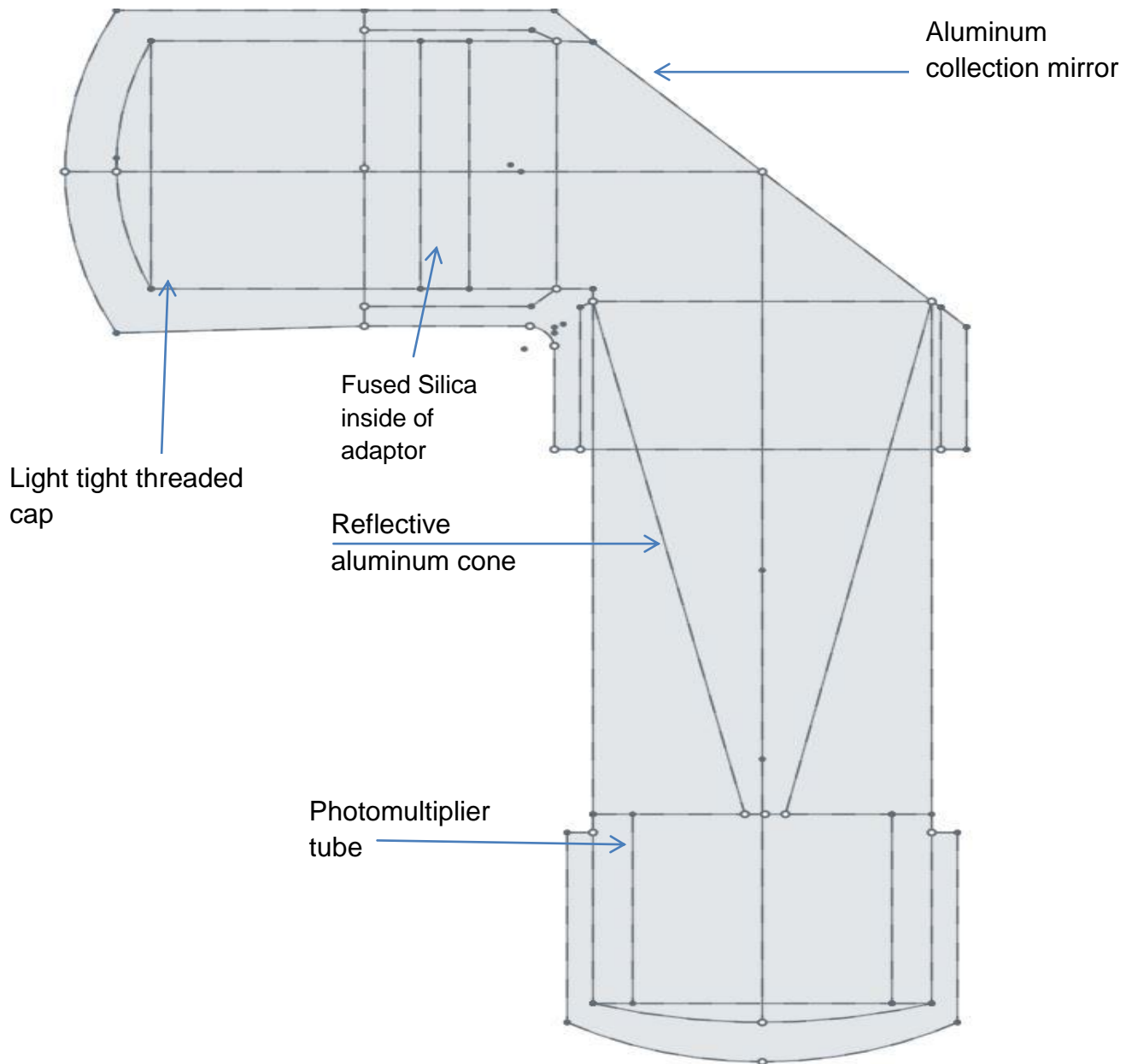
Figure 2: OnShape modeled Cherenkov detector with labels indicating where important parts are located. The detector was designed using 3" schedule 80 PVC parts with the specs from [4] and a 75 mm diameter fused silica piece.

In order to ensure that all of these constraints were met and to test different configurations, the CAD software OnShape [5] was used to model detector designs. Schedule 80 PVC [4] was the material chosen for the detector construction since it is a durable, non-reflective material. The detector had to be light tight so that external light would not affect the system and alter measurements taken on the oscilloscope. In order to meet this constraint, threaded light-tight caps were added to the front and the bottom of the detector. The photomultiplier tube (PMT) had to be easily interchangeable so that different PMTs, such as ones that were micro-channel plates with different size housings, could be used. This was done by adding a threaded mount on the bottom of the detector that the PMT housing would attach to. The collection mirror had to be easily accessible so that when it gets worn it can be easily and quickly swapped out with a new one. For this, a 45 degree cut was made in the PVC elbow connector, as shown in figure 2, for attaching and accessing the collection mirror, which was then attached by an adhesive to the PVC. A polished aluminum cone was added inside the bottom PVC piece as shown in figure 2 to control the path of Cherenkov light and to ensure that the PMT will be able to detect this light. Finally, an adapter was added near the front of the detector to allow for the input of different-size pieces of glass since different materials would be tested using this detector and those pieces might not all be the same size. The piece tested had 12 mm thickness and 75 mm diameter. These dimensions were chosen since they would give the largest measurable wavelengths for Cherenkov radiation based on theoretical calculations and simulations. Figure 2 shows a fused silica piece used during initial tests in place of quartz.

3.2 Detector manufacturing and assembly

From the CAD drawing done in OnShape, the detector was built and prepared for testing by LLE mechanical engineers. The assembly process was also modeled by LLE mechanical engineers and shows how all of the parts fit together. An exploded-view diagram is shown in figure 3. Once the detector was built, the quartz was cleaned and black tape was added to seams and bolt holes to reduce external light and to make the detector closer to being truly light tight. A rubber gasket was also added on top of the PMT to ensure that no light could enter the system through that opening in the bottom of the detector.

1. PMT housing
2. Housing clamp
3. Rubber gasket
4. 3" PVC elbow connector
5. 3" PVC piece
6. 3" PVC piece
7. Cherenkov guard
8. Aluminum mirror
9. Aluminum cone
10. PMT adapter
11. Quartz
12. Photek PMT
13. Light tight guard
14. Light tight cap
15. Bolts for housing
16. Bolts for PMT adapter
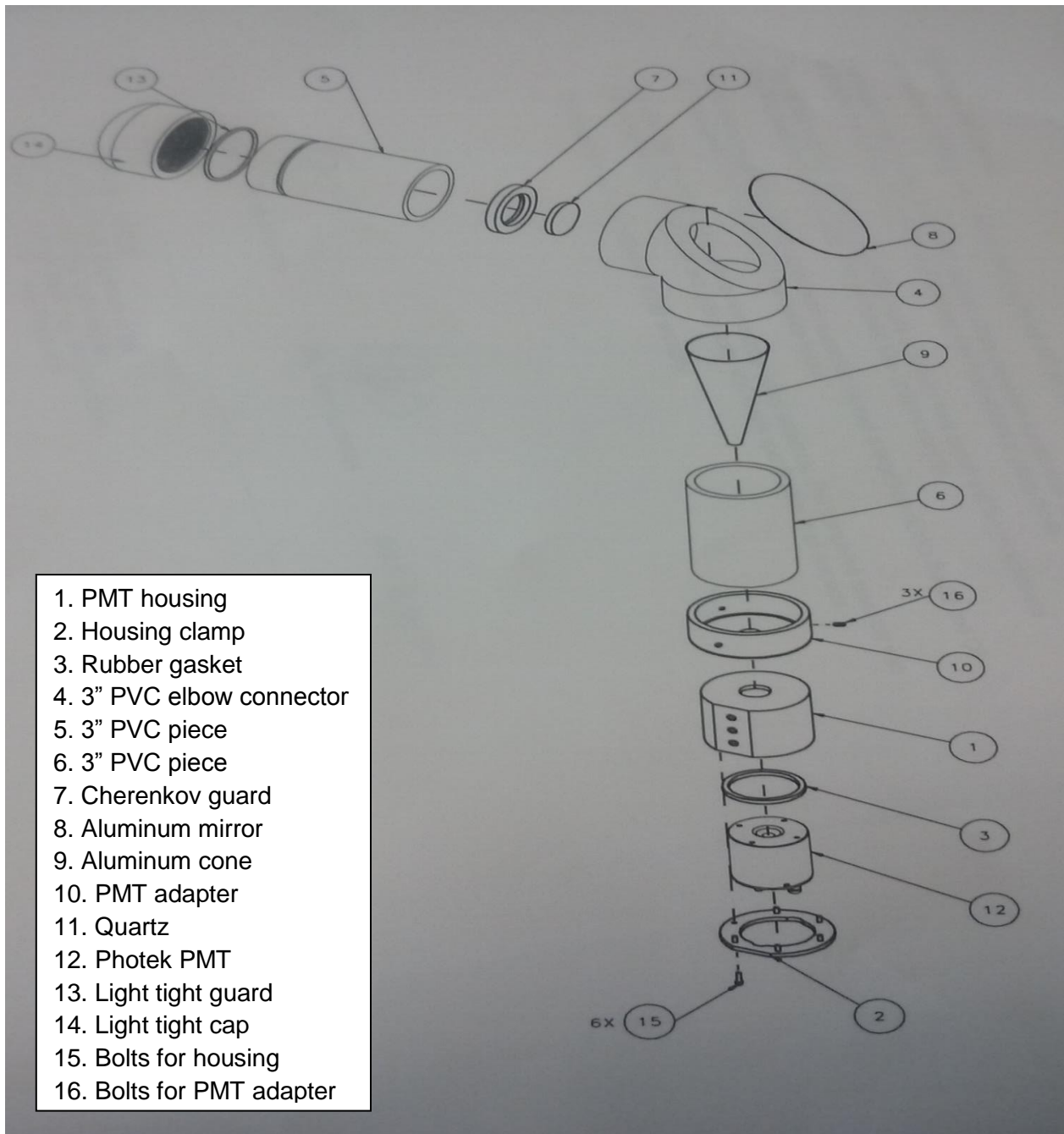
Figure 3: An exploded view of the assembly drawing of the modeled Cherenkov detector with a callout box of the different components.

3.3 Detector theoretical calculations and simulations

To estimate the signal in the detector, the first step is to calculate the signal voltage V_β arising from a single particle (relativistic electron) with a speed of βc, where c is the speed of light in vacuum. This signal is given by the equation:

$$V_\beta = \frac{q_e}{\delta t_{PMT}} \cdot L_{SiO_2} \cdot 50\Omega \cdot \Omega_{PMT} \cdot \int \frac{\partial^2 N_{Cherenkov}(\beta,\lambda)}{\partial x \partial \lambda} \cdot R_{M1}(\lambda) \cdot R_{M2}(\lambda) \cdot QE_{PMT}(\lambda) \cdot d\lambda \ . \tag{1}$$

where:

- V_β is the voltage measured for a single particle;

- q_e is the charge of the electron (in Coulombs);

- δt_{PMT} is the response time of the PMT;

- L_{SiO_2} is the thickness of the Cherenkov radiator;

- 50Ω is the input impedence of the signal digitizer;

- Ω_{PMT} is the solid angle fraction of the PMT;

- $\dfrac{\partial^2 N_{Cherenkov}(\beta,\lambda)}{\partial x \partial \lambda}$ is the number of Cherenkov photons emitted per distance x

  traveled through the medium per wavelength λ and is referred to as the spectral intensity of light emitted by the charged particle;

- R_{M1} and R_{M2} are the reflectivities of mirrors 1 and 2; and

- QE_{PMT} is the quantum efficiency of the PMT cathode (the number of electrons produced divided by the number of incident photons).

Recalling that Cherenkov radiation is emitted only when the particle is moving faster than the speed of light in the medium that it is passing through, i.e., c/n where n is the refractive index, it is necessary to calculate n as a function of λ over the wavelength range of interest. For the purposes of the tests reported here, this is 0.2 to 0.9 µm based on information from fused silica such as the observable wavelength of Cherenkov radiation at various thicknesses. The refractive index for fused silica is given as a function of λ by the Sellmeier equation [6]

$$n^2 - 1 = \frac{0.6961663\lambda^2}{\lambda^2 - 0.0684043^2} + \frac{0.4079426\lambda^2}{\lambda^2 - 0.1162414^2} + \frac{0.8974794\lambda^2}{\lambda^2 - 9.896161^2}$$

(2)

The spectral intensity is given by [7]:

$$\frac{\partial^2 N_{Cherenkov}(\beta, \lambda)}{\partial x \partial \lambda} = 2\pi\alpha \left(1 - \frac{1}{\beta^2 n^2}\right) * \frac{1}{\lambda^2}$$

(3)

and determines the strength of the Cherenkov signal over the wavelength range. Here α is the fine structure constant (1/137). Eq. 3 only applies if v> c/n. The right-hand side of Eq. 3 goes to zero when v=c/n. As shown in figure 4, the signal is strongest at shorter wavelengths and has a quick falloff at larger wavelengths.

d²N/dxdλ(photons/μm²)* vs Wavelength
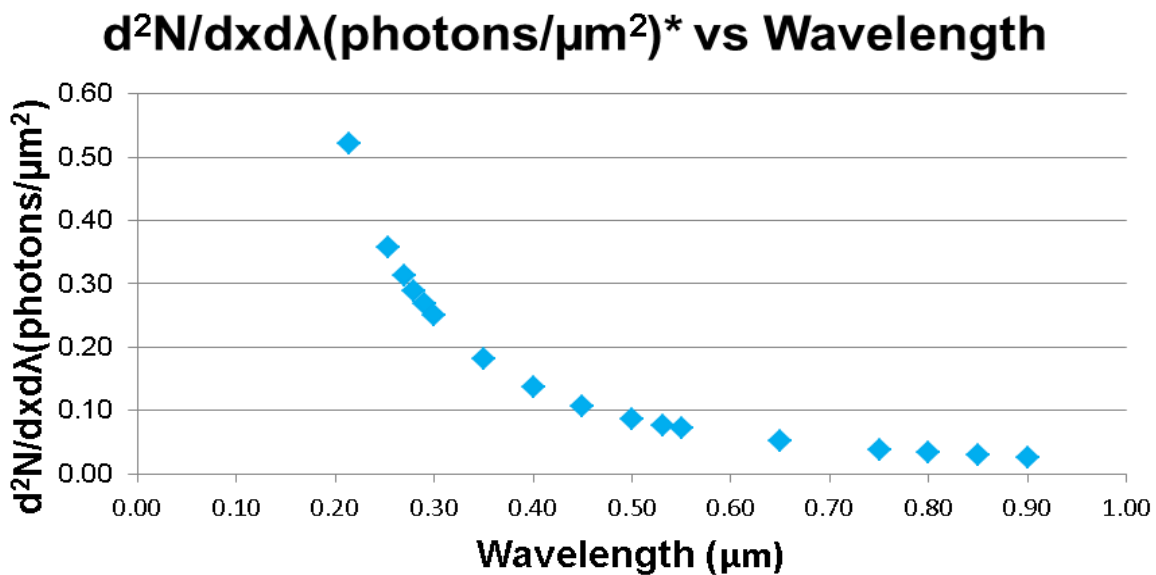
Figure 4: Graph of strength of Cherenkov signal vs wavelength for the range of 0.2 to 0.9 μm. Its shape shows a stronger signal at shorter wavelengths.

The reflectivities of the polished aluminum mirrors R_{M1} and R_{M2} (assumed equal) were found from [8]. Any data missing from the wavelength range was interpolated from the existing data set until a set of data values from 0.2 to 0.9 μm with an interval of 0.05 μm was created.

The solid angle fraction of the PMT gives the fraction of emitted light that is incident on the PMT, and is equal to $A/4\pi L^2$ where A is the aperture area and L is the distance from the emission. This fraction is only $1.2*10^{-4}$. If 100% of the Cherenkov photons were detected, a signal of 0.006 nC would be obtained with the PMT having a gain specified in [9], generating a maximum signal of 82 mV. Taking into account the solid angle fraction, the maximum observable signal per relativistic electron is just 0.01 mV.

The total signal in the detector is calculated by determining the number of relativistic electrons that result from an incident neutron. This was modeled using the Monte Carlo code NRESP7 [7]. This code, developed by G. Dietze and H. Klein, allows the neutron response function to be found for incident-particle energies of 0.05 to 20 MeV. The Monte Carlo output gives the number, energy, and direction of relativistic electrons per incident neutron. The expected signal $V_{neutron}$ is given by:

$$V_{neutron} = \sum_{\beta \geq \frac{1}{n}} S_{MonteCarlo}(\beta, KE_{neutron}) \cdot V_{\beta} \tag{4}$$

where $S_{MonteCarlo}$ is the number of relativistic electrons produced per neutron, a function of β and the neutron kinetic energy $KE_{neutron}$. The summation is only over electrons that will emit Cherenkov radiation.

4. Cosmic ray experiment

4.1 Freestanding experiment

The first experiment that was performed involved using the detector in a freestanding way as shown in figure 5. Muons from cosmic rays can be used to interact with the Cherenkov detector giving a measureable voltage signal which will show that the detector is working. When this experiment was performed, however, the detector only ended up measuring background radiation from the detector noise and thus did not actually detect any radiation put into the detector or any signal emitted from the fused silica. Signal levels of at least 10 mV from the detector would be needed to provide a measurable signal.

4.2 Cosmic ray telescope experiment

In order to correct for the signal not being detected by the detector, a cosmic ray telescope was constructed for the second experiment with the experimental setup shown in figure 6. Scintillation detectors were placed above and below the Cherenkov detector. The motivation behind this experiment was that if a signal is detected in both the top and bottom scintillator that means that a cosmic ray passed through the Cherenkov detector and therefore that a signal should be recorded by the scope. The scintillators in this setup simply act as detection amplifiers so the cosmic ray can be found by the scope. This setup was tested with an applied voltage of 4900 V to the PMT and the signal was then recorded on the oscilloscope. The oscilloscope had 4 channels on it where channel 1 was connected to the detector to record cosmic ray pulses, channels 2 and 3 were hooked up to the top and bottom scintillators to amplify the cosmic ray, and channel 4 was not connected. This oscilloscope output file was later analyzed with MATLAB codes that calculate the pulse height. The MATLAB code was written specifically to interpret scope data and to create output graphs that are human readable so the data can be easily analyzed. When the data was extracted with this code, the result was a noise signal generated from the PMT as shown in figure 7. The noise signal from the PMT is 0.2 mV and is still 20 times the expected single particle voltage of 0.01 mV.
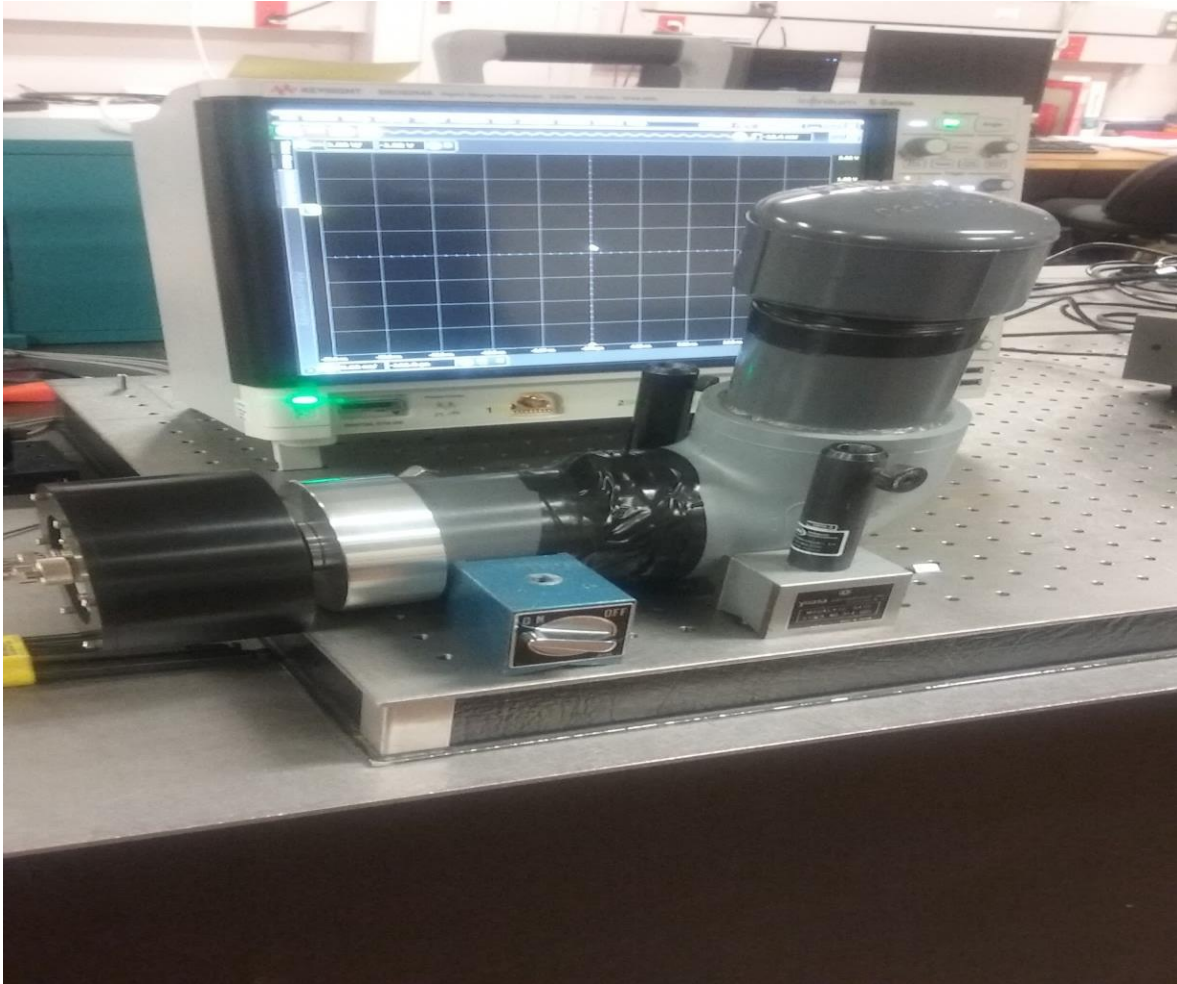
Figure 5: First experimental setup using a free-standing detector. This detector only measured background radiation and noise and no actual cosmic rays.
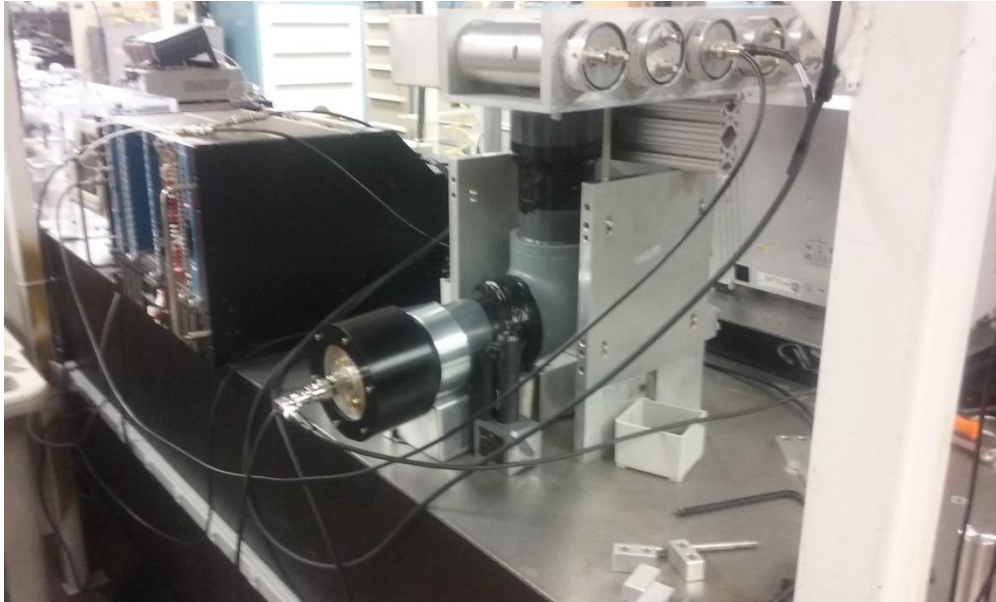
Figure 6: Second experimental setup involving a cosmic ray telescope. If a cosmic ray is detected in the top and bottom scintillator, then that signal will be recorded. The scintillators in the setup are mirrored on the bottom and only one is connected on each of the top and bottom.
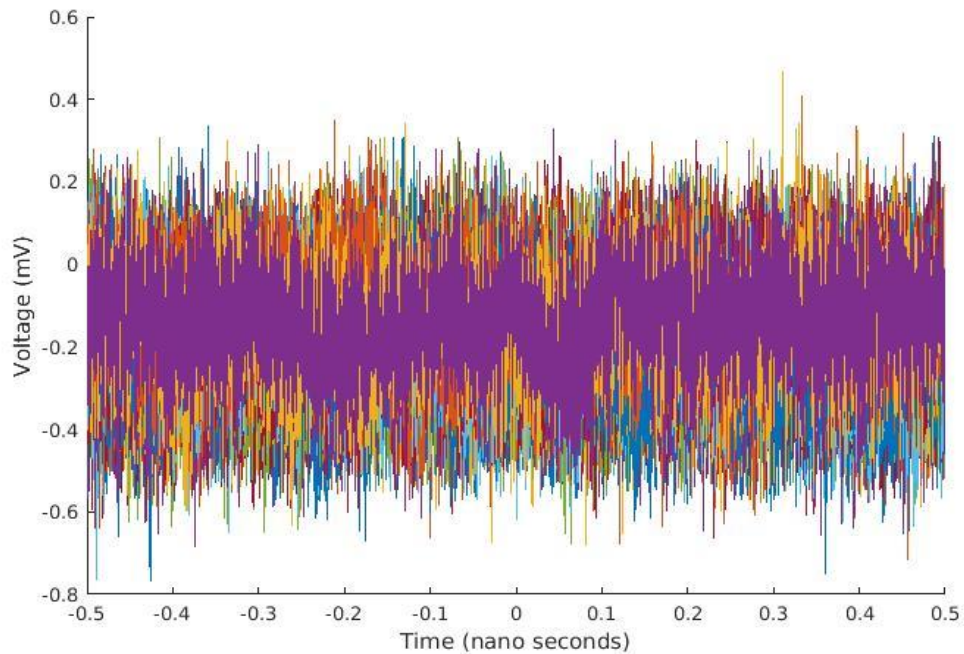
Figure 7: Example output graph from scope data during the second cosmic ray test. The scope shows only noise, which means that a cosmic ray was not detected.

5. Conclusions

A Cherenkov detector was successfully designed, built, and tested. However, when the detector was tested with single particles it was found that it only picked up background noise. One way to address this issue is to make the detector larger in order to be able to pick up a larger signal. Also, the detector efficiency could be improved by decreasing the amount of signal that is lost and the strength of the Cherenkov signal could be increased by passing the particles through a medium where more radiation is created.

The next test will involve putting the detector where it can measure neutrons from a target implosion. Target implosions generate around 10^{14} neutrons that are emitted into 4π steradians. A 75 mm fused silica absorber mounted 5 m from the center of the target chamber will have $1.8*10^{10}$ incident neutrons, resulting in a signal well above the measured noise.

This work will help to get closer to the end goal of being able to reduce the rise time in nTOF experiments and to provide a more accurate measurement of DT and DD neutron pulses with the use of a Cherenkov detector.

6. Acknowledgements

7. References

[1]. B. von Krosigk, L. Neumann, R. Nolte, S. Röttger, K. Zuber, Measurement of the proton light response of various LAB based scintillators and its implication for supernova neutrino detection via neutrino-proton scattering

[2]. C.A.Haynam et al. "National Ignition Facility laser performance status," Appl. Opt. **46**, 3276 (2007).

[3]. Hadiseh Alaeian, An Introduction to Cherenkov Radiation
(http://large.stanford.edu/courses/2014/ph241/alaeian2/)

[4]. Aetna Plastics Corp., pp.14
(https://www.aetnaplastics.com/site_media/media/attachments/aetna_product_aetnaproduct/204/PVC%20Sch%2040%20Fittings%20Dimensions.pdf)

[5]. OnShape Documentation
(https://www.onshape.com/about-us)

[6]. Refractive index information (fused silica)
(https://refractiveindex.info/?shelf=glass&book=fused_silica&page=Malitson)

[7]. G.Dietze, H.Klein PTB-Bericht_ND-22 (1982)

[8]. Laser beam products, Mirrors for Lasers, Science, Industry, Reflectivity of Aluminium – UV, Visible and Infrared
(https://laserbeamproducts.wordpress.com/2014/06/19/reflectivity-of-aluminium-uv-visible-and-infrared/)

[9]. Photek, Photomultipliers
(http://www.photek.com/products/photomultipliers.html)